

Use of Small-Angle Neutron Scattering To Study Tubulin Polymers

Dan L. Sackett,[†] Victor Chernomordik,[†] Susan Krueger,[‡] and Ralph Nossal^{*†}

Laboratory of Integrative and Medical Biophysics,
National Institute of Child Health and Human Development, National Institutes of Health,
Bethesda, Maryland 20892, and NIST Center for Neutron Research,
National Institute of Standards and Technology, Gaithersburg, Maryland 20899

Received August 23, 2002; Revised Manuscript Received December 11, 2002

Small-angle neutron scattering has been used to examine taxol-stabilized microtubules and other tubulin samples in both H₂O and D₂O buffers. Measurements were made at pH/pD values between 6.0 and 7.8, and observed scattered intensities, $I(Q)$, have been interpreted in terms of multicomponent models of microtubules and related tubulin polymers. A semiquantitative curve fitting procedure has been used to estimate the relative amounts of the supramolecular components of the samples. At both pH and pD 7.0 and above, the tubulin polymers are seen to be predominantly microtubules. Although in H₂O buffer the polymer distribution is little changed as the pH varies, when pD is lowered the samples appear to contain an appreciable amount of sheetlike structures and the average microtubule protofilament number increases from ca. 12.5 at pD \geq \approx 7.0 to ca. 14 at pD \approx 6.0. Such structural change indicates that analysis of microtubule solutions based on H₂O/D₂O contrast variation must be performed with caution, especially at lower pH/pD.

Introduction

Small-angle neutron scattering (SANS) and related neutron scattering spectroscopic techniques have special attributes that make them attractive tools for examining complex macromolecular assemblies. Foremost, perhaps, is the opportunity to selectively change the relative scattering intensities from particular components of an assembly by varying the D₂O/H₂O ratio of the buffer. Many multicomponent biological systems are good candidates for this type of analysis because the overall atomic compositions of their individual constituents (proteins, nucleic acids, lipids, etc.) may be sufficiently different that they have intrinsically different neutron scattering characteristics. In other instances functional complexes may be formed by combining natural with artificially perdeuterated components. Applications of such “contrast matching” schemes to biological systems have included studies of nucleosomes¹ and ribosomes,² investigations of hemoglobin within red blood cells³ and neurophysin proteins in secretory vesicles,⁴ and studies of Ca²⁺-mediated protein complexes.^{5,6}

The ubiquitous cytoskeletal proteins actin and tubulin are present within most eucaryotic cells in relatively high concentrations. These molecules polymerize into different forms, both during normal cell function⁷ and when the cells are subject to interventions such as application of antimetabolic drugs in the treatment of cancer.⁸ A large number of proteins interact with actin and tubulin to mediate their roles in cell

division and motility, as well as their involvement as structural determinants of cell shape and scaffolds along which materials are transported from one cellular region to another. Cytoskeletal components also may interact with lipid-containing membranes and intracellular vesicles. Hence, one can envision many instances where one might wish to examine composite systems containing tubulin and/or actin, including in vitro models in which cytoskeletal structures are polymerized within artificial vesicles.^{9,10} Here, in anticipation of using neutrons as probes of the structure and dynamics of such complex cytoskeletal assemblages, we report the scattering cross sections of supramolecular tubulin structures assembled in buffers containing either H₂O or, predominantly, D₂O.

Microtubules (MT) are the most familiar, and biologically most significant, tubulin polymers. Much is known about the various macromolecules that interact with MT in cells to regulate their assembly, structure, and function.⁷ Among these are the “microtubule associated proteins” (MAPs) that bind to the outer surface of a MT and possibly act as bridges between tubulin polymers as well as between MT and other cell components.¹¹ Also, kinases,¹² G-proteins,¹³ and ATP-consuming proteins that act as motors¹⁴ are known to interact with MT. Native cellular MT typically are composed of 13 filaments arranged in a hollow cylinder. The polymer is composed of α - and β -tubulin components, which appear in soluble form as $\alpha\beta$ heterodimers and in protofilaments as alternating $\alpha\beta\alpha\beta$ forms. The polymerization, structure, and supramolecular ordering of tubulin are known to be sensitive to such environmental variables as pH, temperature, solution ionic strength, and ionic character and the presence of tubulin-binding drugs such as taxol.^{15,16}

* To whom correspondence may be addressed: E-mail: rjn@helix.nih.gov.

[†] National Institute of Child Health and Human Development, National Institutes of Health.

[‡] NIST Center for Neutron Research, National Institute of Standards and Technology.

Tubulin polymers have been studied by a variety of physical methods. Many investigations have involved electron microscopy (e.g., ref 17), yet it can be difficult to quantitatively assess solution structures by this surface-adsorbance-based technique. Optical microscopy has been used to study mesoscopic, relatively large-scale behavior such as structural fluctuations linked to mechanical properties,¹⁸ and small-angle X-ray scattering (SAXS) has been used in some studies to obtain information about supramolecular structure on shorter length scales, covering the range of tens to hundreds of angstroms. In particular, recent SAXS studies have provided 30 Å resolution data about the structure of MT in solution at neutral pH, yielding information on the axial center-to-center distance between tubulin monomers and the apparent number of protofilaments in MT formed under differing conditions, e.g., in the presence of taxol and taxol derivatives.^{15,16}

We here report on the structures of taxol–tubulin polymers in buffers of differing hydrogen activity in H₂O and D₂O. These are inferred by fitting scattered intensities to semi-quantitative computational models for samples that contain MT of differing protofilament number as well as varying amounts of sheetlike structures, tubulin oligomers, and unpolymerized $\alpha\beta$ -tubulin dimers. We find that at pH 7.0 or pD 7.0, tubulin polymers are predominantly in the form of MT. However, when the pH or pD of the samples is varied, changes in scattering cross section occur which indicate changes in the constituent polymer forms of the assembly system. Such observations are of intrinsic interest, as they may illuminate basic self-assembly mechanisms of MT and other supramolecular cell structures. Although neutrons have been used to examine the alignment of microtubules within concentrated macroscopic arrays of reconstituted MT,¹⁹ SANS data have not, until now, been systematically related to details of supramolecular structure.

Materials and Methods

Sample Preparation. Tubulin was prepared from rat brains in two steps. Microtubule protein (tubulin + MAPs) was prepared by temperature-driven cycles of polymerization and depolymerization.²⁰ MAP-free tubulin was prepared from this material by selective polymerization of tubulin in 1.6 M MES (2 N morpholinoethanesulfonic acid), pH 6.9, and 1.0 M sodium glutamate as described in detail elsewhere.²¹ Tubulin was adjusted to 50 mg/mL in MME buffer (0.1 M Mes, 1 mM MgCl₂, 1 mM EGTA (ethyleneglycol bis- β -aminoethyl ether *N,N'*-tetraacetic acid), pH 6.9 in H₂O), drop-frozen in liquid nitrogen, and stored in liquid nitrogen. Buffers of differing pH and pD were prepared by NaOH titration of 0.1 M Mes solutions in H₂O and D₂O, respectively, until the desired pH meter reading was obtained. Compensation for the glass electrode response for D₂O solutions was done by the usual correction:²²

$$\text{pD} = (\text{pH meter reading}) + 0.4 \text{ units}$$

Samples for SANS were prepared by dilution of the tubulin stock to 4 mg/mL in the above-mentioned buffers, previously supplemented with 0.1 mM GTP and either MAPs, glutamate,

or taxol, as indicted below. Thus, the “D₂O” samples referred to in this paper actually contain 10% H₂O/90% D₂O.

Small-Angle Scattering and Data Reduction. Small-angle neutron scattering data were obtained at the NG3 30-m CHRNS SANS instrument²³ at the NIST Center for Neutron Research, National Institute of Standards and Technology, Gaithersburg, MD. Neutrons at wavelengths of $\lambda = 5$ Å or $\lambda = 6$ Å, with a wavelength spread of $\Delta\lambda/\lambda = 0.15$, were scattered onto a 64 × 64 cm position-sensitive detector with 1 cm spatial resolution. The source-to-sample and sample-to-detector distances were varied as needed to obtain data in a range $0.008 \text{ \AA}^{-1} \leq Q \leq 0.27 \text{ \AA}^{-1}$, where $Q = 4\pi \sin(\theta/2)/\lambda$ and θ is the scattering angle. It was found that the range $0.01 \text{ \AA}^{-1} \leq Q \leq 0.1 \text{ \AA}^{-1}$ was generally sufficient to ascertain the overall structural parameters and morphology of a solution of tubulin polymers. Sample temperature, ranging from 7 to 35 °C, was maintained with a cooling bath attached to the sample block.

Raw data were corrected for background and detector efficiency as described,²³ using the scattering from the solvent alone as the “empty” cell run. The data were placed on an absolute scale by comparing the scattered intensity directly to the flux incident on the sample. Circular averaging produced scattered intensity, $I(Q)$, vs Q . Residual isotropic “background” scattering, due to hydrogen in the tubulin samples themselves, was removed by fitting the flat portion of the data at higher Q and subtracting the result from $I(Q)$ at all Q values. Finally (except as noted), the data were “desmeared”, i.e., corrected for the wavelength spread and angular divergence of the neutron beam, using a Gaussian resolution function having Q and angular variances as given in Glinka et al.²³

Simulated SANS Intensities. To obtain scattering functions for comparison with data, SANS intensities were simulated using Monte Carlo methods as described in Hansen.²⁴ For each putative constituent of the scattering assembly, a model of supramolecular structure was constructed from volume elements of suitable size and shape. The molecular volume associated with this structure was randomly filled with points, and an interpoint distance distribution function, $P(r)$, was approximated by calculating the frequency of point-to-point distance, r , for all points in the volume. The scattered intensity, $I(Q)$, then was obtained by a simple Fourier transformation of $P(r)$.

MT were modeled (Figure 1) by hollow cylinders, each constructed of a three-start helix formed from tubulin monomers such that the latter provide a continuous wall for the MT.^{15,16,25} The mean cross-sectional radii, which varied in accordance with the number of protofilaments in the MT, were obtained from X-ray diffraction results for 13-protofilament MT²⁶ and cryoelectron microscopy results for MT consisting of varying numbers of protofilaments.²⁷ We allowed the number of protofilaments n_f to vary between 11 and 14 (the validity of which is confirmed by our analysis of SANS data), and we used, as values of mean helical radii, $R = 102, 110, 118, \text{ and } 127 \text{ \AA}$ for $n_f = 11, 12, 13, \text{ and } 14$, respectively. Upon taking the value of the vertical distance (rise) between $\alpha\beta$ dimers along the protofilament to be $p \approx 80 \text{ \AA}$ and using the simple formula²⁵ $P = Sp/2$, where $S =$

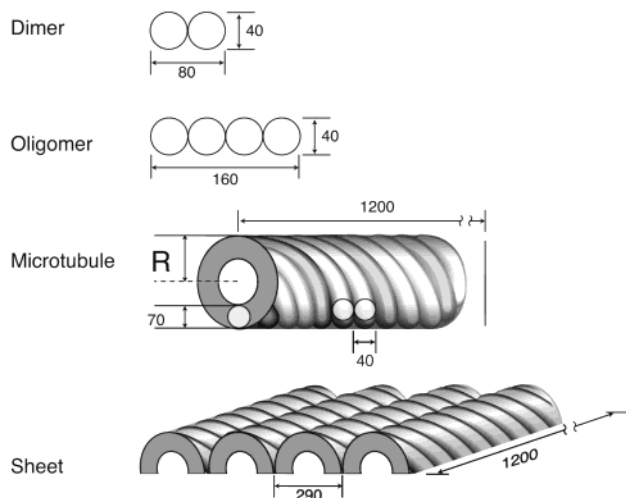


Figure 1. Depiction of structures comprising the scattering assembles used when fitting SANS data. (All lengths given in Å.) The principal component is microtubules (MT), here chosen to be of length 1200 Å, which is sufficiently long that length effects become unimportant for the Q values probed in these SANS experiments (see text). The basic units of a MT are $\alpha\beta$ -tubulin heterodimers, represented here as paired spheres. On a nanoscopic scale, MT structure is that of a three-start helix having the form of three identical interwoven, elliptical coils (see text) whose diameter equals that of one tubulin molecule (40 Å). Helicity results from the slight offset, along the long axis of the MT, of one dimer with respect to its circumferential neighbor. Only one dimer is shown here in the diagram of the MT, but the end-to-end linear association of dimers along the axis of the MT forms a protofilament. The number of protofilaments determines the radius R . We allow a variable distribution of protofilament numbers and account for free dimers as well as possible small aggregates (“oligomers” consisting of two tubulin dimers in a linear array). Included, also, are “sheets” consisting of four contiguous substructures, each of which is a three-start helix sliced in half.

3 is the assumed helix start number, we estimated the value of the pitch P for the start helices to be ≈ 120 Å. This value of the helical pitch agrees well with that considered by Andreu et al.,^{15,16} viz., $P = 123.3$ Å. The minor start-helix radius, determining the thickness of the microtubule wall, was assumed to be 35 Å in accordance with the dimensions of the tubulin monomers forming the wall.

We did not take into account the fine structure of individual monomers within the polymers, since our analysis here is limited to larger scale effects related to the number of protofilaments and the mass fraction of MT “sheets” (or “open” MT). These MT “sheets” were modeled by four collinear half-microtubules (each being a 12-protofilament microtubule cut along its axis), where the center-to-center distance between the half-microtubules is 290 Å. Since the lengths of the MT and “sheets” are greater than the sizes that can be measured in the Q range accessible to these experiments, several different lengths L were investigated in order to ascertain the minimal length needed to fit the data with the computational model. Lengths of 1200 Å or greater were found to match the scattered intensities best. That is, in the Q range observed, the expected intensity profiles from MT of different lengths greater than 1200 Å become negligibly different. However, it is worth noting that even lengths as short as 300 Å were sufficient to reproduce the maxima (but not intensity distributions) in the scattered intensity profiles correctly. We have chosen $L = 1200$ Å in

order to efficiently carry out the Monte Carlo simulations. Finally, the basic building block of the polymers, which we refer to as the “monomer” but which in fact is a tubulin heterodimer consisting of α and β subunits, was simply modeled as two identical, attached spheres, each of 20 Å radius (i.e., a structure of cross-sectional radius 20 Å and length 80 Å). A tubulin “oligomer” was similarly modeled as four linearly stacked spheres.

Determination of Assembly Constituents. To determine the likely polymer composition of the samples from the desmeared, circularly averaged SANS data, we applied a curve-fitting procedure based on the standard Levenberg–Marquardt method.²⁸ A linear combination of the simulated scattering amplitudes pertaining to the various polymeric components described above was fitted to our experimental data. Coefficients of this combination, used as free fitting parameters, provided estimates of relative abundance of the assembly constituents in the samples. A similar procedure has recently been used to analyze time-resolved light scattering data.²⁹

Our analysis demonstrates clear differences in the polymerization of tubulin solutions in H_2O and D_2O that vary consistently as a function of pH (pD). As usual with such a curve fitting procedure, it cannot be strictly shown from a mathematical point of view that any particular combination of coefficients is the only adequate solution. However, over a broad range of assumed initial values of the fitting parameters, final results of iterations prove to be practically identical. As shown in the analysis and discussion section below, the fits obtained are quite good. Note, though, that we limit our analysis here to the range of scattering vectors $0.05 \text{ \AA}^{-1} < Q < 0.1 \text{ \AA}^{-1}$, which provides information of the large scale structure of the MT polymers. Consideration of data for higher values of Q ($0.1 \text{ \AA}^{-1} < Q < 0.2 \text{ \AA}^{-1}$) is required to estimate fine-scale structural details of the microtubules, but such details have not been included in the present models.

Results

Figure 2 shows SANS cross sections, $I(Q)$, for tubulin polymerized in different solution conditions. All are in 90% D_2O , pD 7.0, and all contain 0.1 mM GTP. Each panel presents the data obtained after polymerization at 35 °C and, also, after subsequent cooling to 7 °C from 35 °C. The data given in Figure 2A were obtained from samples containing tubulin and microtubule associated proteins (MAPs). In the sample whose cross section is shown in Figure 2B, polymerization took place in 1 M sodium glutamate, while in Figure 2C polymerization occurred in the presence of excess taxol.

Well-defined peaks are seen in Figure 2C and, to a lesser extent, in the 35 °C data of parts A and B of Figure 2. These peaks correspond to broad scattering rings which are visible in the raw data at an angle corresponding to $Q \sim 0.03 \text{ \AA}^{-1}$. However, the precise position of the peak maximum seems to vary slightly with sample conditions, which may indicate differences in mean microtubule diameter or the presence of incomplete MT in the form of tubulin oligomers (see Figure 6 and the analysis and discussion section). Other

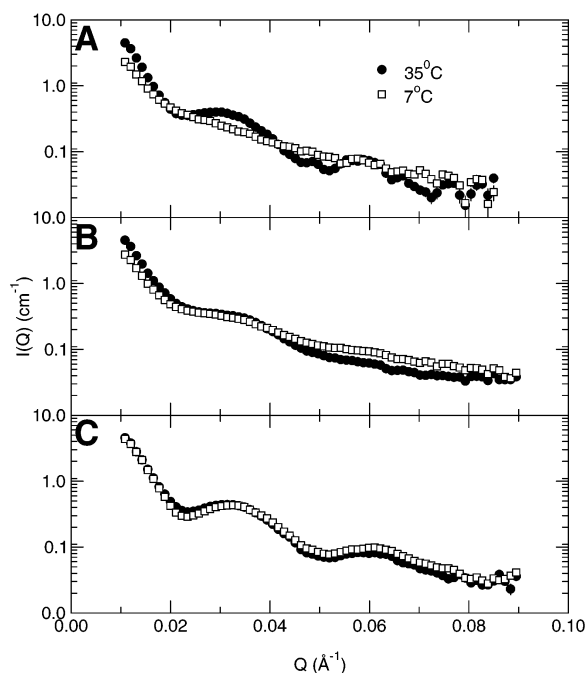


Figure 2. Relative scattered intensities are shown for (A) tubulin + MAPs, (B) tubulin in 1 M sodium glutamate, and (C) tubulin-taxol. All samples contain 90% D₂O, 1 mM GTP, and 4 mg/mL protein and are at pD 7.0. Samples were allowed to polymerize at 35 °C after which data were collected. The samples then were cooled to 7 °C, and measurements were repeated. (Data shown here have not been desmeared.)

interesting features are the secondary maxima at $Q \sim 0.06 \text{ \AA}^{-1}$ and the relative peak amplitudes and overall slopes of the cross sections.

The effects of cooling the samples to 7 °C are also shown in Figure 2. As seen in Figure 2C, cooling the taxol-polymerized tubulin sample had little effect on the scattering. This is expected, given the known stabilization of MT by this agent. In contrast, in parts A and B of Figure 2 the prominent peaks seen in the 35 °C data are less visible after cooling. The tubulin plus MAPs data shown in Figure 2A indicate a major structural change—probably considerable depolymerization—after cooling. Interestingly, a significant amount of “cold-stable” polymer appears to remain in the glutamate sample (Figure 2B).

In anticipation of making use of the “contrast matching” capability of SANS, we compared scattering in D₂O- and H₂O-based solutions. Figure 3 compares $I(Q)$ for tubulin-taxol in the two buffer systems. In Figure 3A, we show the desmeared data for D₂O, pD 7.0, compared with the calculated intensity for a mixture of MT containing 12, 13, and 14 protofilaments in the mass ratio 1.25:0.69:0.0005 (for discussion of the calculations, see Methods and Figure 6). In Figure 3B, we show the same data for D₂O compared with desmeared data from an H₂O sample at pH 7.0. Two points emerge from the comparison: (1) The data quality is good from both, although the H₂O data are slightly noisier at $Q > \sim 0.1 \text{ \AA}^{-1}$ (this is not evident as presented in the figure); and (2) at pH/pD = 7.0, the scattering cross sections are qualitatively very similar.

The assembly of MT and the interaction with other proteins is known to be pH dependent,³⁰ so we varied the pH or pD

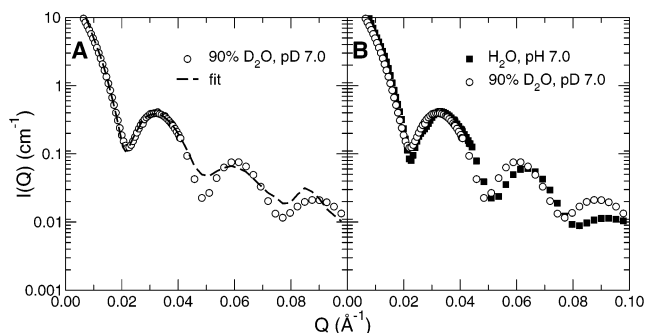


Figure 3. Scattered intensities for tubulin-taxol in D₂O and H₂O: (A) desmeared scattering cross sections for tubulin-taxol in 90% D₂O at pD 7.0 compared with computed cross sections for a mixture of 12-, 13-, and 14-protofilament MT (in the mass ratio 1.25:0.69:0.0005); (B) desmeared scattering cross sections for tubulin-taxol in 90% D₂O pD 7.0, and in H₂O pH 7.0, are shown, illustrating that the data are similar at pD/pH 7.0 and that good scattering is obtained from MT in both D- and H-based solutions.

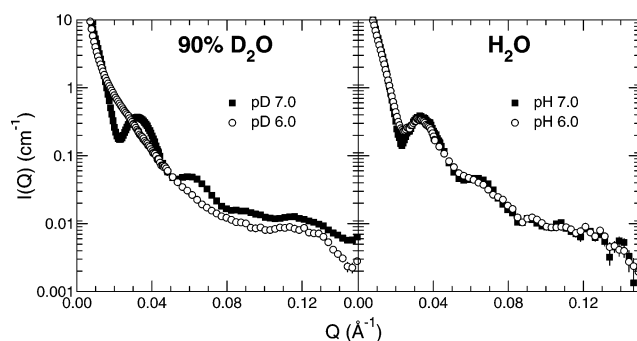


Figure 4. Effect of changes in pH and pD on scattering cross sections. Desmeared data for tubulin-taxol samples in 90% D₂O (left) are compared with H₂O samples (right) at pH/pD 7.0 or 6.0.

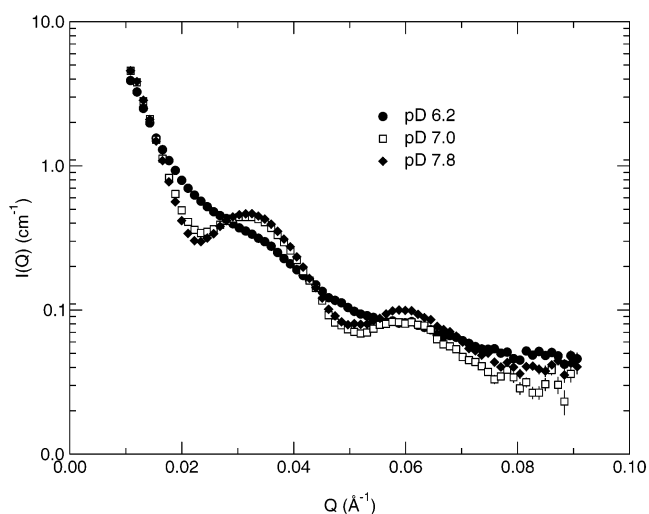


Figure 5. Desmeared data for tubulin-taxol samples in 90% D₂O are compared at pD 7.8, 7.0, and 6.2.

of the buffer. In Figures 4 and 5 we show the effect of pH/pD variation on the scattered intensities. Figure 4 presents desmeared data from tubulin-taxol samples at pD or pH 7.0 compared with pD or pH 6.0. Unlike the case at pH/pD 7.0, the cross sections are quite different when samples are assembled at pH/pD 6.0. In H₂O, the features of $I(Q)$ in both the pH 7.0 and pH 6.0 samples are similar, while in D₂O there are marked differences. Figure 5 demonstrates that the gross changes observed at pD below 7.0 are not observed

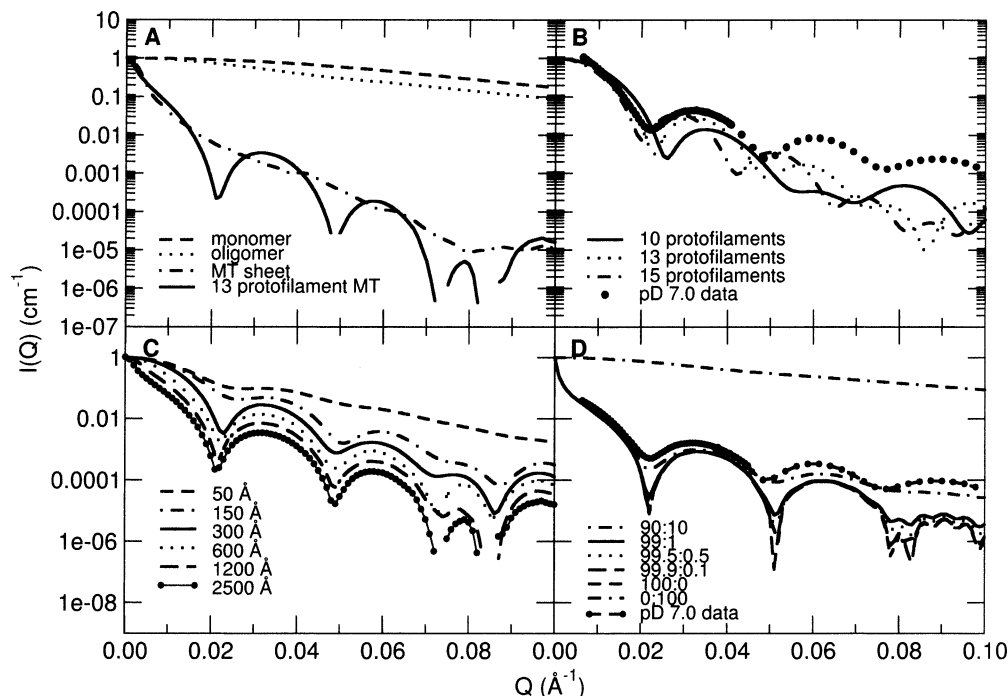


Figure 6. Model calculations showing how MT parameters affect the relative scattered intensity, $I(Q)$: (A) calculated intensities for tubulin “monomer” (the dimer, which is the basic unit of higher order polymers), a four-unit “oligomer”, sheets, and 13-protofilament MT (sheet and MT lengths are 1200 Å); (B) the effect of changing protofilament number compared with desmeared data on tubulin–taxol pD 7.0 (MT lengths are 300 Å). (C) the effect of MT length on scattering from 13-protofilament MT; (D) the effect of mixing differing amounts of oligomer (top curve) with 13-protofilament MT (bottom curve), compared with desmeared tubulin–taxol pD 7.0 data (large dots).

above pD 7.0, i.e., the cross sections at pD 7.8 and pD 7.0 differ only slightly, while even at pD 6.2 the large change seen in Figure 4 is already evident. Similarly the cross sections at pH 7.8 and pH 7.0 are identical (data not shown).

Analysis and Discussion

For the polymerization conditions used here, observations from electron micrographs indicate that at pH 7.0 tubulin + MAPs polymers, as well as tubulin–taxol polymers, will be MT into which almost all of the tubulin has been incorporated. However, tubulin–taxol samples have also been shown to contain small amounts of sheetlike and ribbonlike polymers at other pH values,³⁰ as do glutamate–tubulin samples.³¹

To what extent can one distinguish among these structures when analyzing a SANS experiment? To address this question, we simulated $I(Q)$ for various presumed scattering assemblies as described in Materials and Methods (see Figure 1). Illustrative results of model calculations for α,β -tubulin dimers, MT, and sheetlike entities are shown in Figure 6A. In Figure 6B, the effect of changes in the protofilament number on the scattering of MT is shown, demonstrating that the position of the first minimum is sensitive to the average protofilament number. The desmeared data for the pD 7.0 tubulin–taxol sample at 35 °C are presented for comparison. Figure 6C illustrates the effect of polymer length. The calculated cross sections contain oscillations whose maxima occur at values of Q , which are invariant with polymer length when the latter is at least equal to the external diameter of the (cylindrical) polymer (in this case, ≥ 300 Å). Although oscillation amplitudes and overall slope

do seem to depend on cylinder length, this dependence is not strong, so we conclude that the length of the MT is an indeterminate variable whose exact value is unimportant if the MT are long enough. This is not surprising, since the Q -range accessible in these experiments corresponds to length scales consistent with the cross-sectional diameter of the MT, not their total length, which can exceed the diameter by more than an order of magnitude.

In Figure 6D we show how the presence of tubulin structures other than MT might affect the scattered intensity. As an example, we show in this panel calculated cross sections for various mixtures of oligomers and 13-protofilament MT. We also plot the desmeared data for the pD 7.0 tubulin–taxol sample at 35 °C for comparison. It is of interest that the presence of even relatively small mass fractions of “monomer” or “oligomer” can result in a discernible straightening and smoothing of $I(Q)$ at larger values of Q . The calculations support the notion that, at pD 7.0, the samples are almost all polymerized—and that the small amount of polymer other than MT is likely to be in the form of short oligomers.

Using this model, we fitted mixtures of the various polymer forms to the data. The computational procedure, which is detailed in Materials and Methods, provides good fits for samples containing MT having differing protofilament number and varying amounts of oligomers, dimers, and MT sheets. Although we obtained data from a number of samples in D₂O and H₂O at many values of pD and pH, we limit our analysis here to data for which the pH/pD is 7.0 or lower since it is in that range that changes in observed cross sections are most apparent. In Figure 7 we show results,

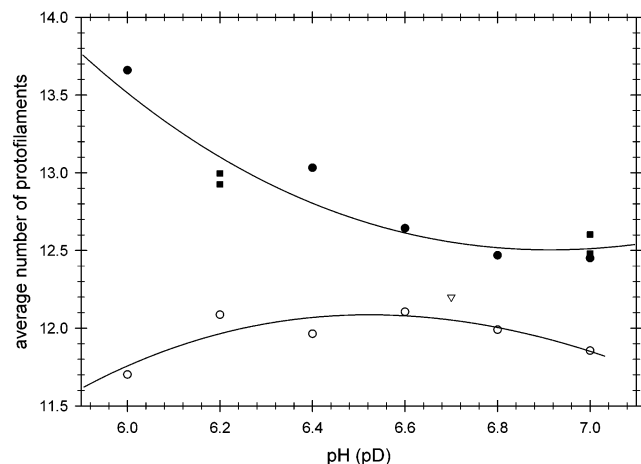


Figure 7. The effect of changing the pH or pD on the protofilament number of MT. Tubulin–taxol samples were prepared in buffers of the indicated pH or pD, polymerized at 35 °C, and data collected and processed as described in Materials and Methods. The desmeared data were analyzed for the presence of polymers of different character as discussed in the text. The average protofilament number of the MT polymers in the fit is plotted versus the pH (pD) of the sample. D₂O samples are filled symbols while H₂O samples are open symbols. Results from two sets of measurements (circles and squares) are shown, to indicate repeatability of the data and analysis. The triangle represents data from a similar SAXS study of MT in H₂O.¹⁶

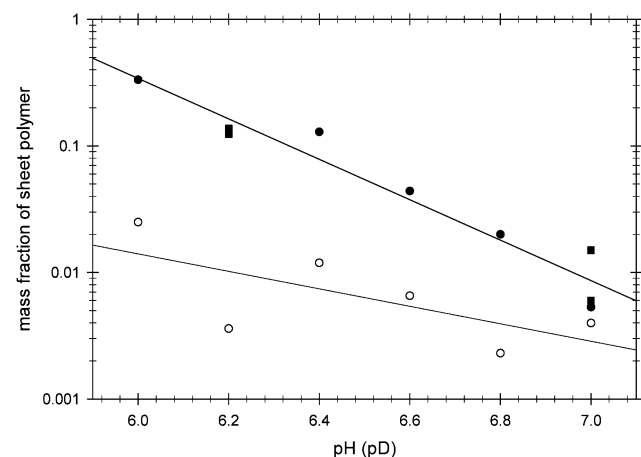


Figure 8. The effect of changing the pH or pD on the mass fraction of sheet polymers. Data are from the same fits used to obtain the results in Figure 7, and the symbols have the same meaning. The mass fraction of sheet polymers is shown for both D₂O and H₂O samples.

focusing on the modifications in protofilament number for the MT polymers present.

Due to the assumptions used in our analysis, in certain respects our treatment must be considered to be only semiquantitative in nature, but there clearly is little change in the H₂O samples. Moreover, we find that the retrieved average protofilament number is in good agreement with that previously reported based on SAXS data at pH 6.7.¹⁶ In contrast, in D₂O protofilament number is not constant, but increases as pD is decreased from 7.0. The difference between D₂O and H₂O samples is reinforced by the results given in Figure 8, which indicate for the D₂O samples a significant increase in the mass fraction of the sample present as MT sheets when pD was decreased. In H₂O, however, the amount of sheet structures remain low at all pH values.

Additionally, the present study shows that substitution of D₂O for H₂O alters tubulin polymer structure, even in the presence of taxol, and that these differences are affected by variation of pH/pD. At pH or pD values near 7.0, the polymers observed are almost all MT, but the D₂O and H₂O samples differ in that D₂O polymers consistently have a slightly larger diameter, indicating a larger number of protofilaments. Taxol is known to lower the average protofilament number from 13 to close to 12,¹⁶ and the data of Figure 7 show good agreement with the earlier X-ray data. In D₂O, however, the average protofilament number is closer to 13. As pD is lowered, the protofilament number increases further, to about 14 at pD 6. Only small changes are observed in H₂O samples upon variation of pH.

Other investigators have demonstrated that, in addition to structure, the dynamics of MT formation are changed by D₂O.³² Also it has been noted that tubulin is protected by D₂O from spontaneous inactivation at both 4 and 37 °C and that polymerization of tubulin in D₂O containing 8% DMSO yields sheetlike ribbon polymers.³³ In contrast, MT are formed in H₂O in the presence of similar amounts of DMSO. Taken together, these results are of considerable interest, as several studies have demonstrated that high concentrations of D₂O can be cytotoxic to mammalian cells,³⁴ presumably due to inhibition of mitosis (discussed in ref 35). This perturbation of the cell cycle is probably linked to changes in the polymerization of MT, as lower concentrations are known to affect the spindle volume (discussed in ref 32).

Several other reports also have demonstrated that the *in vitro* properties of protein molecules can be altered by the presence of D₂O. For example, the conformational stability of β -lactoglobulin is increased by D₂O,³⁶ and assembled poliovirus capsid particle is protected against heat- or high-pH-induced dissociation by D₂O and MgCl₂.³⁷ Polymerization of actin,³⁸ flagellin,³⁹ recA,⁴⁰ tobacco mosaic virus protein,⁴¹ and tubulin^{32,42,43} have all been shown to be promoted and stabilized by D₂O. Final polymer form can also be altered; e.g., polymerization of fibrin is similar in D₂O and H₂O, but the D₂O gel has a higher degree of lateral association.⁴⁴

Tubulin polymerization is an entropy-driven process. Water molecules that are ordered by hydrophobic surfaces of the tubulin dimer have increased conformational freedom when those surfaces are buried upon polymerization. Hence, it is plausible that the reported promotion of polymerization in D₂O is due primarily to enhanced hydrophobic interactions (as suggested by Itoh and Sato⁴³). This is understandable at the molecular level from an analysis of the structure of the tubulin dimer and its docking into the high-resolution structure of the microtubule.⁴⁵ The latter study reveals that the protein surfaces involved in longitudinal contact between dimers, responsible for elongation of the MT, are mainly hydrophobic, with minimal electrostatic interactions. Therefore, enhancement of hydrophobic interactions by D₂O can be expected to promote linear extension of MT, that is, longitudinal growth of protofilaments.

However, it is not clear how the mechanism referenced above would result in an increase in protofilament number, or a pD-dependent protofilament number. Since the protofil-

ament number and sheet fraction increased as pD was lowered from 7 to 6, whereas such change was not seen in H₂O, it seems likely that these changes are due either to enhancement of hydrogen bonding between protofilaments or to D₂O effects on pH-dependent H⁺ dissociation from some residue(s) involved in lateral interaction of protofilaments. This is supported by the chemical nature of the surfaces involved, as lateral contacts have an important ionic component, unlike longitudinal contacts which are dominated by hydrophobic interactions.⁴⁵ A problem with this explanation is that the shift in H⁺ dissociation behavior of protein residues in D₂O is expected to be of the order 0.4–0.5 pH units upward,⁴⁶ so, if a simple shift in dissociation were the explanation, the protofilament number and sheet fraction observed at pD 6.4 should be the same as that seen at pH 6.0. Further work will be required to understand the origins of these differences.

Finally, although the possibility of varying D₂O/H₂O to contrast match the components of a biological assembly makes neutron scattering a powerful technique, our results suggest that substitution of D₂O for H₂O in structural studies of proteins should be done with some care. If the structure of the scattering medium remains invariant when D₂O is substituted for H₂O, the solution match point for each of the components of a multicomponent system can be determined separately by plotting the square root of the $Q = 0$ limit of the scattering cross section, $I(0)^{1/2}$, as a function of D₂O concentration and estimating the value of D₂O for which the intensity vanishes. Such a procedure is valid for the tubulin polymers examined in this study when pH/pD is close to 7.0, for which we obtain an approximate value for the match-point D₂O concentration of 40%. Then, after the match points of the individual constituents of a supramolecular complex are determined, the scattering functions for the various interacting components can be determined by measuring the scattering at several different D₂O/H₂O ratios and, as long as the composite structure does not change as the solutions are varied, employing an appropriate linear regression routine to separate the scattered intensities. As has been indicated in the analysis of a two-component protein complex consisting of partially deuterated troponin C and nondeuterated troponin I, scattering measurements from samples in as few as three different buffers could suffice to determine the individual scattering functions.⁵ One might wish to use a similar procedure to study tubulin interacting with, e.g., perdeuterated peptides but, as seen from the results of the present study, more complicated experimental and analysis methods would be required, particularly for samples at lower pH/pD where the relative amounts of microtubules and sheetlike structures seem to vary with D₂O/H₂O.

Acknowledgment. The authors warmly thank Dr. Hacene Boukari for interesting discussions about this and related topics. This work was partially supported by the National Science Foundation under agreement DMR-9423101. The support of the National Institute of Standards and Technology, U.S. Department of Commerce, in providing the neutron facilities used in this work is gratefully noted.

References and Notes

- (1) Pardon, J. F.; Worcester, J. F.; Wooley, J. C.; Tatchell, K.; van Holde, K. E.; Richards, B. B. *Nucleic Acids Res.* **1975**, *2*, 2163.
- (2) Koch, M. H. J.; Stuhmann, H. B. *Methods Enzymol.* **1979**, *59*, 670.
- (3) Krueger, S.; Nossal, R. *Biophys. J.* **1988**, *53*, 97.
- (4) Krueger, S.; Lynn, J. W.; Russell, J. T.; Nossal, R. *J. Appl. Crystallogr.* **1989**, *22*, 546.
- (5) Olah, G. A.; Rokop, S. E.; Wang, C. L.; Blechner, S. L.; Trehwella, J. *Biochemistry* **1994**, *33*, 8233.
- (6) Krueger, J. K.; Zhi, G.; Stull, J. T.; Trehwella, J. *Biochemistry* **1998**, *37*, 13997.
- (7) Alberts, B.; Johnson, A.; Lewis, J.; Raff, M.; Roberts, K.; Walter, P. *Molecular Biology of the Cell*, 4th ed.; Garland Science: New York, 2002.
- (8) Sackett, D. L.; Fojo, T. *Cancer Chemother. Biol. Response Modif.* **1999**, *18*, 59.
- (9) Kuchnir-Fygenson, D.; Elbaum, M.; Shraiman, B.; Libchaber, A. *Phys. Rev. E* **1997**, *55*, 850.
- (10) Boulbitch, A.; Simson, R.; Simson, D. A.; Merkel, R.; Hackl, W.; Barmann, M.; Sackmann, E. *Phys. Rev. E* **2000**, *62*, 3974.
- (11) Black, M. M. *Proc. Natl. Acad. Sci. U.S.A.* **1987**, *84*, 7783.
- (12) Crute, B. E.; Van Buskirk, R. G. *J. Neurochem.* **1992**, *59*, 2017.
- (13) Roychowdhury, S.; Wang, N.; Rasenick, M. M. *Biochemistry* **1993**, *32*, 4955.
- (14) Vale, R. D.; Reese, T. S.; Sheetz, M. P. *Cell* **1985**, *42*, 39.
- (15) Andreu, J. M.; Bordas, J.; Diaz, J. F.; Garcia de Ancos, J.; Gil, R.; Medrano, F. J.; Nogales, E.; Pantos, E.; Towns-Andrews, E. *J. Mol. Biol.* **1992**, *226*, 169.
- (16) Andreu, J. M.; Diaz, J. F.; Gil, R.; de Pereda, J. M.; Garcia de Lacoba, M.; Peyrot, V.; Briand, C.; Towns-Andrews, E.; Bordas, J. *J. Biol. Chem.* **1994**, *269*, 31785.
- (17) Unger, E.; Bohm, K. J.; Vater, W. *Electron Microsc. Rev.* **1990**, *3*, 355.
- (18) Hotani, H.; Miyamoto, H. *Adv. Biophys.* **1990**, *26*, 135.
- (19) Tabony, J.; Job, D. *Nature* **1990**, *346*, 448.
- (20) Sackett, D. L.; Knipling, L.; Wolff, J. *Protein Expression Purif.* **1991**, *2*, 390.
- (21) Wolff, J.; Sackett, D. L.; Knipling, L. *Protein Sci.* **1996**, *5*, 2020.
- (22) Glasoe, P. K.; Long, F. A. *J. Phys. Chem.* **1960**, *64*, 188.
- (23) Glinka, C. J.; Barker, J. G.; Hammouda, B.; Krueger, S.; Moyer, J. J.; Orts, W. J. *J. Appl. Crystallogr.* **1998**, *31*, 430.
- (24) Hansen, S. *J. Appl. Crystallogr.* **1990**, *23*, 344.
- (25) Metoz, F.; Wade, R. H. *J. Struct. Biol.* **1997**, *118*, 128.
- (26) Mandelkow, E.; Thomas, J.; Cohen, C. *Proc. Natl. Acad. Sci. U.S.A.* **1977**, *74*, 3370.
- (27) Wade, R. H.; Cretien, D. *J. Struct. Biol.* **1993**, *110*, 1.
- (28) Press, W. H.; Teukolsky, S. A.; Vetterling, W. T.; Flannery, B. P. Cambridge University Press: New York, 1997.
- (29) Chenomordik, V.; Hattery, D.; Gannot, I.; Gandjbakhche, A. H. *IEEE J. Sel. Top. Quantum Electron.* **1999**, *5*, 930.
- (30) Ringel, I.; Horwitz, S. B. *J. Pharmacol. Exp. Ther.* **1991**, *259*, 855.
- (31) Hamel, E.; del Campo, A. A.; Lowe, M. C.; Waxman, P. G.; Lin, C. M. *Biochemistry* **1982**, *21*, 503.
- (32) Panda, D.; Chakrabarti, G.-a.; Hudson, J.; Pigg, K.; Miller, H. P.; Wilson, L.; Himes, R. *Biochemistry* **2000**, *39*, 5075.
- (33) Chakrabarti, G.; Kim, S.; Gupta, M. L.; Barton, J. S.; Himes, R. H. *Biochemistry* **1999**, *38*, 3067.
- (34) Fischer, A. *Protoplasma* **1936**, *26*, 51.
- (35) Krendel, M.; Inoue, S. *Biol. Bull.* **1995**, *189*, 204.
- (36) Verheul, M.; Roefs, S. P. F. M.; de Kruif, K. G. *FEBS Lett.* **1998**, *421*, 273.
- (37) Chen, C.-H.; Wu, R.; Roth, L. C. G.; Guillot, S.; Crainic, R. *Arch. Biochem. Biophys.* **1997**, *342*, 108.
- (38) Omori, H.; Kuroda, M.; Naora, H.; Takeda, H.; Nio, Y.; Otani, H.; Tamura, K. *Eur. J. Cell Biol.* **1997**, *74*, 273.
- (39) Uratani, Y. *J. Biochem.* **1974**, *75*, 1143.
- (40) Ruigrok, R. W. H.; DiCapua, E. *Biochimie* **1991**, *73*, 191.
- (41) Khalil, M. T. M.; Lauffer, M. A. *Biochemistry* **1967**, *6*, 2474.
- (42) Houston, L. L.; Odell, J.; Lee, Y. C.; Himes, R. H. *J. Mol. Biol.* **1974**, *87*, 141.
- (43) Itoh, T.; Sato, H. *Biochim. Biophys. Acta* **1984**, *800*, 21.
- (44) Larsson, U. *Eur. J. Biochem.* **1988**, *174*, 139.
- (45) Nogales, E. *Cell* **1999**, *96*, 79.
- (46) Kalinichenko, L. P.; Lobyshev, V. P. *Stud. Biophys.* **1976**, *58*, 235.